JOURNAL OF PHYSICAL ORGANIC CHEMISTRY
J. Phys. Org. Chem. 2006; **19:** 503–511
Published online 5 December 2006 in Wiley InterScience (www.interscience.wiley.com). DOI: 10.1002/poc.1049

Ab initio calculations of the gas-phase elimination kinetics of ethyl oxamate, ethyl oxanilate, and ethyl *N*,*N*-dimethyl oxamate†

Jose R. Mora,[1] Marcos Loroño,[1] Tania Cordova[2]* and Gabriel Chuchani[3]

[1]Departamento de Química, Escuela de Ciencias, Universidad de Oriente Núcleo Sucre, Cumana, Venezuela
[2]Escuela de Química, Facultad de Ciencias, Universidad Central de Venezuela, Apartado 1020-A, Caracas,Venezuela
[3]Centro de Química, Instituto Venezolano de Investigaciones Científicas (I.V.I.C.), Apartado 21827, Caracas,Venezuela

Received 29 September 2005; revised 23 December 2005; accepted 06 February 2006

ABSTRACT: Theoretical studies of the gas-phase elimination kinetics of title compounds were performed by using "*ab initio*" methods at MP2/6-31G, MP2/6-31G(d,p) and ONIOM [MP2/6-31G (d,p) // MP2/6-31G]. Ethyl Oxamate and ethyl oxanilate undergo a rapid decarbonylation to give the corresponding carbamates. These intermediates proceed to a parallel decomposition to give the corresponding unstable carbamic acid and ethylene through six-membered cyclic transition state (path 1) and isocyanate and ethanol through a four-membered cyclic transition state (path 2). Ethyl *N*,*N*-dimethyloxamate elimination reaction yields in one step, through a six-membered cyclic transition state, dimethyl oxamic acid and ethylene gas. The calculated bond orders, NBO charges and synchronicity indicate that these reactions are concerted and slightly asynchronous. The estimated kinetic and thermodynamic parameters are in good agreement with the reported experimental values. Copyright © 2006 John Wiley & Sons, Ltd.

KEYWORDS: kinetics; unimolecular elimination; pyrolysis; ethyl oxamate, ethyl oxanilate; ethyl *N*,*N*-dimethyl oxamate; "*ab initio*" calculations; reaction mechanism; transition-state structure

INTRODUCTION

The elimination kinetics of ethyl esters with different substituents at the acid or acyl side had already been described.[1] Kinetic parameters and the comparative rates imply these reactions to proceed through a six-membered cyclic transition state to give the corresponding carboxylic acid and ethylene, respectively [reaction (1)].[1] For molecular elimination it is necessary the presence of a C_β—H bond at the alkyl side of the ester.

These organic esters gave a good Taft–Topsom correlation as shown in Fig. 1.

The negative value of $\rho_\alpha = -0.68$ suggests a modest participation of the polarizability effect or steric effect. The greatest absolute value of $\rho_F - = +2.57$ indicates that the field or electronic effect has the most important influence in the elimination process. The value of $\rho_R{}^- = -1.18$ confirms the interaction of the substituent Z with an incipient negative reaction center and implies a favorable effect for the abstraction of the β-hydrogen of the ethyl ester by the oxygen carbonyl in the transition state.

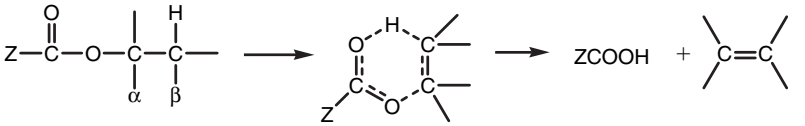

Z=Substituent

(1)

Z = H, CH_3, C_6H_5, $(CH_3)_2N$, $(CH_3CH_2)_2N$, CH_3O, Cl

A recent work[2] on the gas-phase elimination kinetics of ethyl oxamate, ethyl oxanilate, and *N*,*N*-dimethyl oxamate examined the effect of the interposition of a polar group, such as carbonyl, between the nitrogen substituents described in reaction (1) and the acid side of ethyl ester. Ethyl *N*,*N*-dimethyl oxamate without an H atom bonded to N was believed to undergo a concerted

**Correspondence to:* T. Cordova, Instituto Venezolano de Investigaciones, Científicas, Centro de Química Apartado 21827, Caracas 1020A, Venezuela.
E-mail: chuchani@quimica.iic.ve
†Selected paper presented at the 10th European Symposium on Organic Reactivity, 25–30 July 2005, Rome, Italy.

six-membered cyclic transition state type of mechanism [reaction (2)]. The 2-oxo acid intermediate, at the working temperature, is unstable and decarboxylates very rapidly, in a similar step to that observed for pyruvic and benzoyl formic acid[3,4] reaction (3)]. The product of step 2 is dimethylformamide.

The carbamate intermediate from step 1 of reaction (4) undergoes a parallel elimination to isocyanate and ethanol and to the unstable carbamic acid and ethylene gas. Step 2 leads to the formation of an isocyanate perhaps through a concerted four-membered cyclic transition state, while step 3 through a concerted six-membered cyclic transition state yields ethylene and the corresponding carboxylic acid. The unstable carbamic acid may probably decarboxylate by way of a concerted four-membered cyclic transition state type of mechanism.

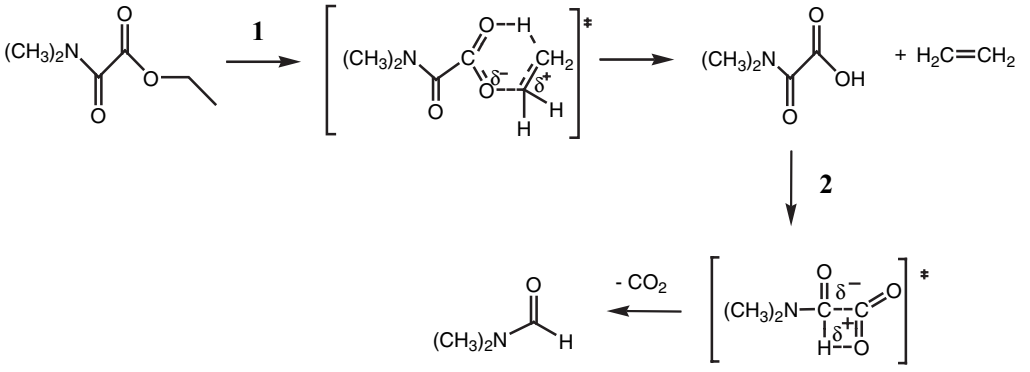

(2)

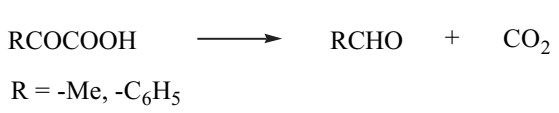

(3)

In the case of ethyl oxamate and ethyl oxanilate, a rapid decarbonylation to the corresponding carbamate is the first step of elimination [reaction (4), step 1]. The mechanism of decarbonylation can be related to a recent publication on the elimination kinetics of methyl oxalyl chloride [reaction (5)].[5]

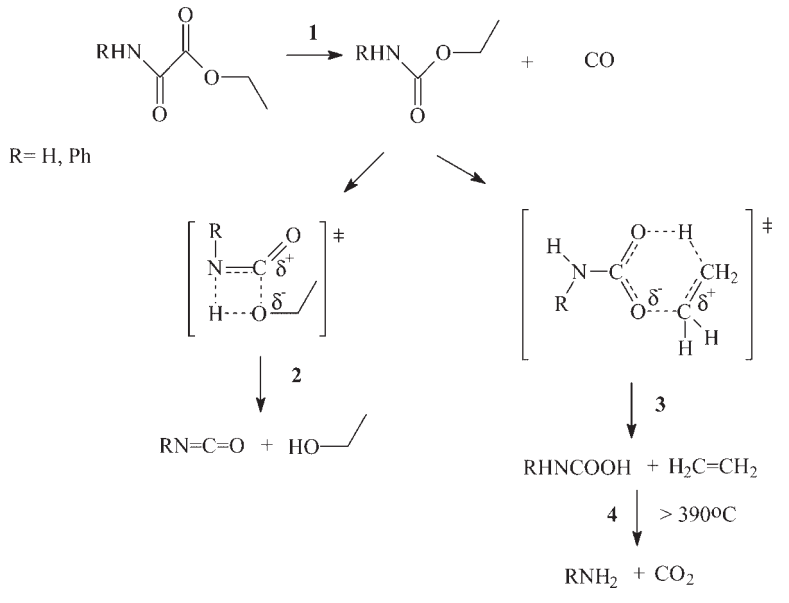

(4)

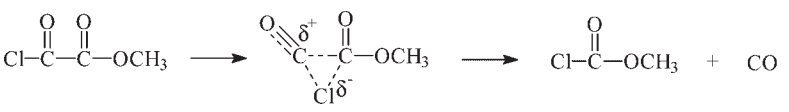

(5)

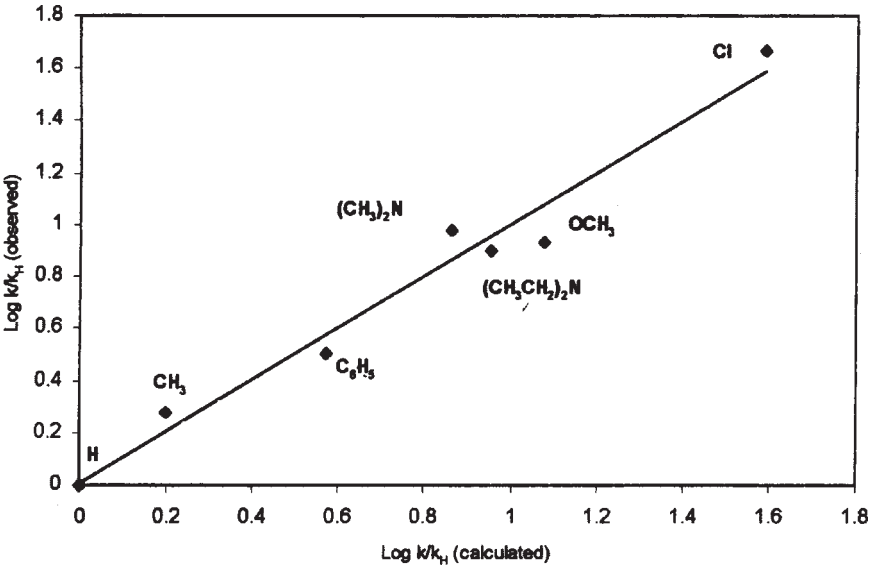

Figure 1. Taft–Topsom correlation for the pyrolysis of $ZCOOCH_2CH_3$ log $k/k_0 = -(0.68 \pm 0.12)\sigma_\alpha \pm (2.57 \pm 0.12)\sigma_F - (1.18 \pm 0.27)\sigma_R^-$.($r = 0.984$, sd = 0.119 at 400°C)

To verify or support the suggested mechanisms for the elimination of the ethyl esters of the oxamic acid described above, we present a theoretical study at the MP2/6-31G level in order to determine the kinetic and thermodynamic parameters of the gas-phase elimination reaction of ethyl oxamate, ethyl oxanilate, and ethyl *N*,*N*-dimethyl oxamate. The thermal decomposition of ethyl oxamate, ethyl oxanilate occurs in three steps processes. The first step is a fast decarbonylation of the substrate to the corresponding carbamate (reaction 4). This carbamate decomposes by two competitive paths to give ethylene and an unstable carbamic acid (path 1) while path 2 produces ethanol and isocyanic acid or its derivative. This latter mechanism does not occur in ethyl *N*,*N*-dimethyl oxamate, because it lacks of a hydrogen atom on the nitrogen. Consequently, this substrate decomposes through path 1 to yield ethylene and *N*,*N*-dimethyl oxamic acid. This intermediate decarboxylates to give dimethyl formamide.[2]

COMPUTATIONAL METHODS AND MODELS

The gas-phase elimination kinetics and mechanisms of ethyl oxamate, ethyl oxanilate, and ethyl *N*,*N*-dimethyl oxamate were investigated by means of electronic structure calculations using Møller–Plesset perturbation method (MP2) with 6-31G, 6-31G(d,p) basis set and ONIOM [MP2/6-31G // MP2/6-31G(d.p)] as implemented in Gaussian 98W.[6] Since both ethanol and ethylene formation were observed for ethyl oxamate, ethyl oxanilate, both path 1 and 2 were studied. In the case of ethyl *N*,*N*-dimethyl oxamate calculations were performed for path 1.

Structures for reactants, products, and transition states were optimized at MP2 with 6-31G, 6-31G(d,p) basis set and ONIOM [MP2/6-31G // MP2/6-31G(d,p)] levels of theory. The Berny analytical gradient optimization routines were used. The requested convergence on the density matrix was 10^{-9} atomic units, the threshold value for maximum displacement was 0.0018 Å, and that for the maximum force was 0.00045 Hartree/Bohr. The nature of stationary points was established by calculating and diagonalizing the Hessian matrix (force constant matrix). TS structures were characterized by means of normal-mode analysis. The transition vector (TV) associated with the unique imaginary frequency, that is, the eigenvector associated with the unique negative eigenvalue of the force constant matrix, has been characterized.

Thermodynamic quantities such as zero point vibrational energy (ZPVE), temperature corrections $E(T)$ and absolute entropies $S(T)$, were obtained by frequency calculations and consequently, the rate coefficient can be estimated assuming that the transmission coefficient is equal to 1. Temperature corrections and absolute entropies were obtained assuming ideal gas behavior from the harmonic frequencies and moments of inertia by standard methods[7] at average temperature and pressure values within the experimental range. Scaling factors for frequencies and zero point energies for MP2 methods used are taken from the literature.[8]

The first-order rate coefficient $k(T)$ was calculated using the TST[9] and assuming that the transmission coefficient is equal to 1, as expressed in the following relation:

$$k(T) = (KT/h)\exp(-\Delta G^{\#}/RT)$$

where $\Delta G^{\#}$ is the Gibbs free energy change between the reactant and the transition state and K, h are the Boltzman and Plank constants, respectively.

$\Delta G^{\#}$ was calculated using the following relations:

$$\Delta G^{\#} = \Delta H^{\#} - T\Delta S^{\#}$$

and,

$$\Delta H^{\#} = V^{\#} + \Delta(\mathrm{ZPVE}) + \Delta E(T)$$

where $V^{\#}$ is the potential energy barrier and Δ(ZPVE) and $\Delta E(T)$ are the differences of ZPVE and temperature corrections between the TS and the reactant, respectively.

Frequency calculations were carried at the average experimental conditions (Temperature = 400°C), at the same level of theory used for optimization. Thermodynamic quantities such as ZPVE, temperature corrections ($E(T)$), energy, enthalpy, and free energies were obtained from vibrational analysis. Entropy values were calculated from vibrational analysis and using Chuchani–Cordova[10] idea of factor C^{exp}.

RESULTS AND DISCUSSIONS

Kinetic and thermodynamic parameters

The gas-phase thermal decomposition of ethyl oxamate and ethyl oxanilate occurs by two competitive pathways. In the case ethyl *N*,*N*-dimethyl oxamate there is no hydrogen present at the carbamate nitrogen, therefore, the four member ring TS-II mechanism is precluded, thermal decomposition of this substrate occurs only by path 1 to give ethylene and *N*,*N*-dimethyloxamic acid in a slow step, followed by rapid decarboxylation of the acid to yield *N*,*N*-dimethyl formamide. In this investigation we performed calculations for all possible paths to procure additional evidence on the nature of these mechanisms and the proposed transition state structures.

Results from MP2 calculations for the rate-controlling step are shown in Table 1. The theoretical thermodynamic parameters $\Delta H^{\#}$, $\Delta G^{\#}$, $\Delta S^{\#}$ are in good agreement with experimental. For ethylene formation from ethyl oxanilate, better results were obtained with MP2/6-31G(d,p) and ONIOM [MP2/6-31G // MP2/6-31G(d,p)], with enthalpies and free energies of activation within 4-5 kJ/mol from experimental counterparts. Calculated energies of activation and rate coefficients are also within experimental values. For ethanol formation from ethyl oxanilate, better energy of activation was obtained with MP2/6-31G(d,p). In the case of ethylene formation from ethyl oxamate, best activation parameters were obtained with MP2/6-31G, while for ethanol formation from the same substrate both MP2/6-31G and MP2/6-31G(d,p) gave good results. Ethylene formation from ethyl *N*,*N*-dimethyl oxamate better results were obtained with MP2/6-31G. In general, MP2/6-31G level of calculation gave reasonable agreement with experimental parameters for the substrates under study, while not always the use of polarized functions improved the results.

In the case of ethyl oxanilate (Table 1, X = Ph), the preferred kinetic product is ethanol, with a smaller energy of activation, in accord with experimental determinations. Ethyl oxamate (Table 1, X = H) thermal decomposition the calculated MP2/6-31G* rates by paths 1 and 2 as well as calculated energies of activation are similar for both paths. At MP2/6-31G(d,p) ethanol formation is favored in accord with experiment. Theoretical results for ethyl *N*,*N*-dimethyl oxamate thermal decomposition (path 1) are in good agreement with experimental for MP2/6-31G method.

Table 1. Kinetics and thermodynamic parameters for thermal decomposition of $XHNCOCOOCH_2CH_3$ (X = H, Ph) by path 1 (ethylene formation) and path 2 (ethanol formation) and thermal decomposition of *N*,*N*-dimethyl ethyl oxamate by path 1, from MP2 calculations at 400°C

Method	10^4k (s^{-1})	E_a (kJmol^{-1})	Log *A*	$\Delta S^{\#}$ (Jmol^{-1}K^{-1})	$\Delta H^{\#}$ (kJmol^{-1})	$\Delta G^{\#}$ (kJmol^{-1})
			Formation of ethylene (X = Ph)			
Experimental	15.6	214.1	13.81	4.36	208.5	205.6
MP2/6-31G	8.2	204.5	13.81	4.31	198.9	196.0
ONIOM	12.6	215.3	13.81	4.31	209.7	206.8
MP2/6-31G(d,p)	8.2	217.7	13.81	4.31	211.5	209.2
			Formation of ethanol (X = Ph)			
Experimental	42.0	205.2	13.55	−0.62	199.6	200.0
MP2/6-31G	244.1	195.4	13.55	−0.59	189.8	190.2
ONIOM	204.1	192.7	13.26	−6.10	187.1	191.2
MP2/6-31G(d,p)	190.1	196.8	13.55	−0.59	191.2	191.6
			Formation of ethylene (X = H)			
Experimental	9.77	195.9	12.19	−26.00	190.3	208.3
MP2/6-31G(d,p)	3.04	214.4	13.12	−8.76	208.8	214.8
MP2/6-31G	2.61	203.2	12.18	−26.74	197.6	215.6
			Formation of ethanol (X = H)			
Experimental	20.0	208.0	13.44	−2.73	202.4	204.2
MP2/6-31G	13.1	209.5	13.38	−3.94	203.9	206.6
MP2/6-31G(d,p)	9.82	209.8	13.58	−6.52	204.2	208.6
			Ethyl *N*,*N*-dimethyl oxamate			
Experimental	10.2	206.8	13.06	−10.0	201.2	207.9
MP2/6-31G(d,p)	0.64	221.2	12.97	−11.6	215.6	223.4
MP2/6-31G	44.7	198.6	13.08	−9.5	193.3	199.7

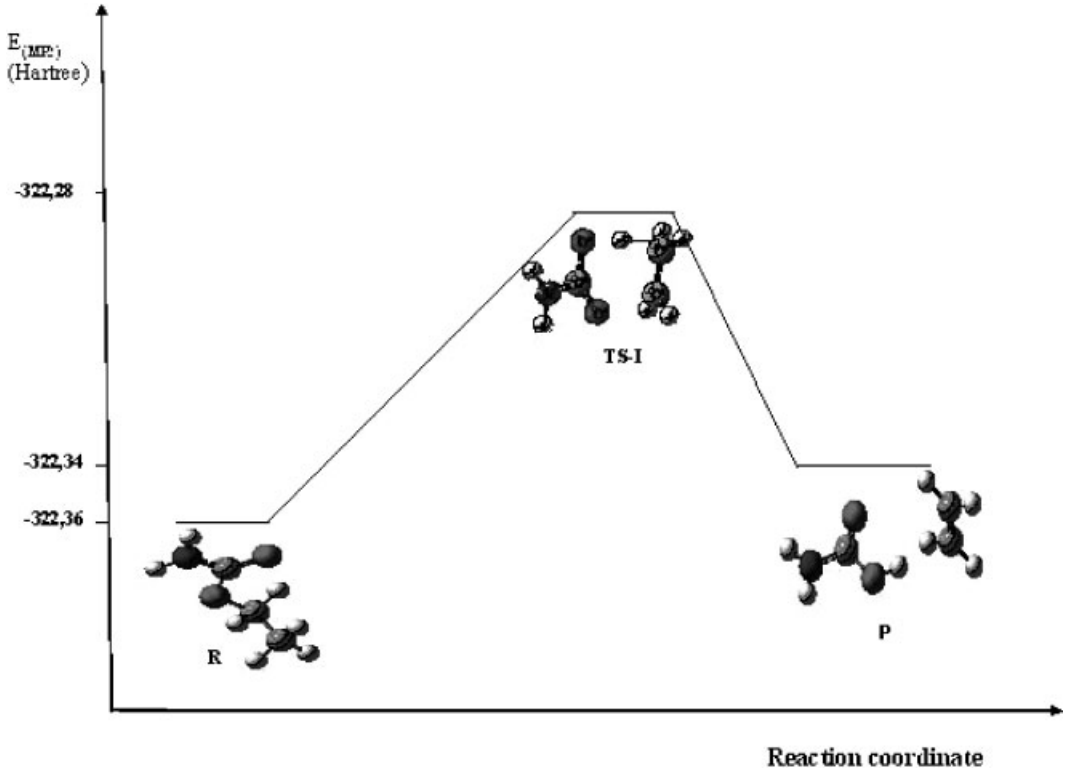

Figure 2. Reaction profile of ethylene formation from ethyl oxamate (path 1). The transition state TS-I is a six-membered ring structure. Paths 1 and 2 are available for ethyl oxamate and ethyl oxanilate, however, for ethyl *N*,*N*-dimethyl oxamate only path 1 is possible due to the substitution on the nitrogen

Calculated rate coefficients for the rate determining step show analogous tendency to that observed experimentally: ethyl oxanilate is more reactive than both ethyl oxamate and ethyl *N*,*N*-dimethyl oxamate, and ethanol formation in the former substrate is the predominant process. This can be explained by an increase hydrogen acidity caused by the electron withdrawing ability of the phenyl group, thus making facile the abstraction of H to oxygen.

Transition states and mechanisms

The gas-phase elimination reaction of ethyl oxamate and ethyl oxanilate occurs by decarbonylation to the corresponding carbamate followed by decomposition in two pathways. The transition state for the rate determining step in path 1 (TS-I), leading to ethylene formation, is a cyclic six-membered structure as suggested by values of log *A* between 12.18 and 13.81.[11] TS-I geometries are similar both in distances and angles between the atoms involved in the reaction (C_3, O_4, O_5, C_6, C_9, and H_{11}) with the hydrogen being transferred (H11) midway between the carbon C_9 and the oxygen O_5 (Fig. 2, Scheme 1). TS-I structures show some departure from planarity as revealed by dihedral angles (maximum deviation 29° and 34°, respectively, Table 2). The process is concerted in the sense that C_6—O_4 and C_9—H_{11} bond distances increase showing breaking of these bonds (1.49–2.01 or 2.03 Å in TS-I and 1.09–1.35 or 1.33 Å in TS-I, respectively). The C_6—C_9 and C_3—O_4 bond distances reveal changes from single to double bond character (1.53–1.41 Å in TS-I and 1.40–1.31Å in TS-I, respectively) as hybridization change from sp3 to sp2. The TV shows that the process is dominated by the elongation of C_6—O_4 bond and the transfer of hydrogen H11 from C9 to O5. Imaginary frequencies for path 1, TS-I for ethyl oxamate and ethyl oxanilate are 1704.0 and 1658.1, respectively (Table 2).

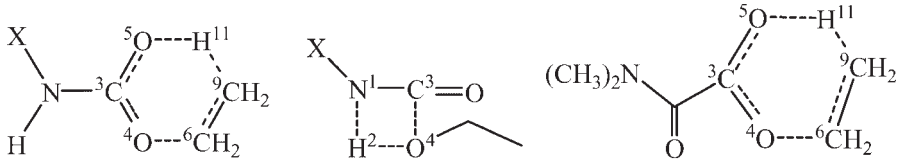

Scheme 1. TS-I: ethylene formation from X = H ethyl oxamate, X = Ph ethyl oxanilate. TS-II: ethanol formation from for X = H ethyl oxamate, X = Ph ethyl oxanilate and TS-I: ethylene formation from ethyl *N*,*N*-dimethyl oxamate

Table 2. Structural parameters for carbamates $XHNCOOCH_2CH_3$ (X = H, Ph) thermal decomposition: reactants (R), TS-I (six-member ring path) and TS-II (four-member ring path), from MP2/6-31G calculations at 400°C. Atom distances are in Å and dihedral angles are in degrees

	H		Ph			H		Ph	
X	R	TS-I	R	TS-I		R	TS-II	R	TS-II
				distances (Å)					
C_3–O_4	1.405	1.313	1.400	1.310	C_3–O_4	1.405	1.793	1.400	1.780
C_3–O_5	1.250	1.320	1.256	1.327	N_1–H_2	1.000	1.360	1.010	1.330
C_6–O_4	1.490	2.010	1.490	2.030	O_4–H_2	2.390	1.190	2.260	1.230
C_6–C_9	1.530	1.410	1.530	1.410	C_3–N_1	1.370	1.310	1.370	1.326
C_9–H_{11}	1.090	1.350	1.090	1.330					
H_{11}–O_5	4.090	1.300	3.960	1.320					
				Dihedral angles					
		TS-I		TS-I			TS-II		TS-II
O_5–C_3–O_4–C_6		28.762		−34.323	O_4–C_3–N_1–H_2		−0.270		−1.785
C_3–O_4–C_6–C_9		−12.360		15.170	C_3–N_1–H_2–O_4		0.430		2.890
O_4–C_6–C_9–H_{11}		−3.080		3.240	N_1–H_2–O_4–C_3		−0.320		−2.260
C_6–C_9–H_{11}–O_5		17.760		−20.460	H_2–O_4–C_3–N_1		0.310		2.240
				Imaginary frequency (cm^{-1})					
		H		Ph			H		Ph
		TS-I		TS-I			TS-II		TS-II
		1704.0		1658.1			1634.1		1560.5

The substrate ethyl *N*,*N*-dimethyl oxamate decomposes only by path 1. The TS-I structure is a six-member cycle comprised by atoms C_3, O_4, O_5, C_6, C_9, and H_{11} as described for ethyl oxamate and ethyl oxanilate. Geometrical parameters are somewhat different, showing more deviation from planarity than the previously described TS-I, as seems from dihedral angles (maximum deviation 58°, Table 3). This departure from planarity may be due to steric hindrance caused by the presence of two methyl groups in the nitrogen. The C_6—O_4 bond breaking shows more extensive change in the TS-I compared to other reaction coordinates. The imaginary frequency associated with the TS-I is 1488.9 cm^{-1}.

The calculated TS-II obtained for path 2, leading to ethanol formation from ethyl oxamate and ethyl oxanilate is a four-membered ring (Fig. 3, Scheme 1), similar for both substrates and very close to planarity as seen in dihedral angles (maximum deviation 0.4°, Table 2, path 2). The C_3—O_4 distance show extensive bond breaking, also breaking is N_1—H_2 bond, while O_4—H_2 bond is forming and C3—N1 is almost a double bond. The TV is associated with the hydrogen transfer from N1 to O4 with an imaginary frequency of 1634.1 and 1560.5 from ethyl oxamate and ethyl oxanilate, respectively.

NBO charge analysis of path 1 for ethyl oxamate, ethyl oxanilate, and ethyl *N*,*N*-dimethyl oxamate revealed that O_4—C_6 bond is highly polarized both in reactants and TS-I structures, in the sense $O_4^{\delta-}$—$C_6^{\delta+}$ (Table 4). From reactant to TS-I, the following changes in partial charges occur: an increase in positive charge $\delta+$ in H11 (from 0.16–0.19 to 0.47–0.48 in TS-I), an increase in negative charge in carbonyl oxygen O5 from −0.63 to −0.77 in TS-I for the first two substrates and from −0.58 to −0.74 for ethyl *N*,*N*-dimethyl oxamate.

Analysis of NBO charges for path 2 for ethanol formation from ethyl oxamate and ethyl oxanilate,

Table 3. Structural Parameters for ethyl *N*,*N*-dimethyl oxamate $(CH_3)_2NCOCOOCH_2CH_3$ thermal decomposition: reactants (*R*) and TS-I (six-member ring) from MP2/6-31G calculations at 400°C. Atom distances are in Å and dihedral angles are in degrees

	C_3–O_4	C_3–O_5	C_6–O_4	C_6–C_9	C_9–H_{11}	H_{11}–O_5
			Distances (Å)			
R	1.394	1.250	1.500	1.520	1.096	3.960
TS-I	1.298	1.320	2.100	1.410	1.310	1.350
			Dihedral angles			
	O_5–C_3–O_4–C_6	C_3–O_4–C_6–C_9	O_4–C_6–C_9–H_{11}	C_6–C_9–H_{11}–O_5		
TS-I	57.88	−31.89	0.720	32.940		
			Imaginary frequency (cm^{-1})			
TS-I			1488.9			

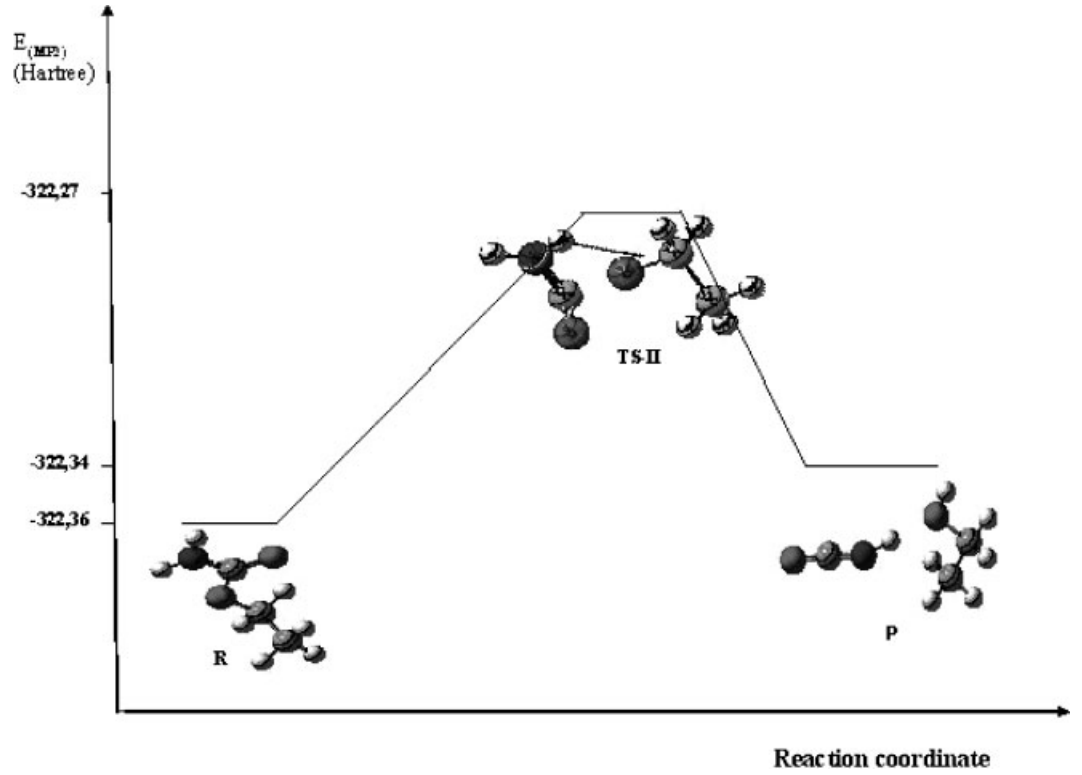

Figure 3. Reaction profile of ethanol formation from ethyl oxamate (path 2). The transition state TS-II is a four-membered cyclic structure. Path 2 is available for ethyl oxamate and ethyl oxanilate

showed strong polarization of C_3—O_4 in the sense $C_3^{\delta+}$—$O_4^{\delta-}$ both in reactants and TS-II structures. This polarization increases in the TS-II for ethyl oxamate (from 1.79 to 1.92), and decrease for ethyl oxanilate (from 1.83 to 1.79) implying assistance of the phenyl group in the stabilization of TS-II. There is also an increase in positive charge for H2 from reactant to TS-II from 0.4 to 0.6 for both substrates.

Bond order analysis

Bond order calculations NBO were performed.[12–14] Wiberg bond indexes[15] were computed using the natural bond orbital NBO program[16] as implemented in Gaussian 98W to further investigate the nature of the TS along the reaction pathway. Bond breaking and making process involved in the reaction mechanism can be monitored by

Table 4. NBO charges for reactants *R*, TS and products *P*, for ethyl oxamate, ethyl oxanilate, and ethyl *N*,*N*-dimethyl oxamate thermal decomposition, from MP2/6-31G calculations at 400°C. Two mechanisms are described for ethyl oxamate and ethyl oxanilate via TS-I (six-member ring) to give ethylene and via TS-II (four-member ring) to give ethanol. Only TS-I type of mechanism is available for ethyl *N*,*N*-dimethyl oxamate

	Ethyl oxamate			Ethyl oxanilate			Ethyl *N*,*N*-dimethyl oxamate		
	R	TS-I	P	R	TS-I	P	R	TS-I	P
O_4	−0.738	−0.745	−0.622	−0.750	−0.743	−0.623	−0.691	−0.650	−0.531
C_3	1.049	1.044	0.994	1.108	1.080	1.047	0.735	0.687	0.678
O_5	−0.628	−0.767	−0.761	−0.629	−0.768	−0.771	−0.577	−0.717	−0.740
H_{11}	0.158	0.479	0.464	0.172	0.474	0.466	0.190	0.456	0.467
C_6	0.007	0.009	−0.362	0.007	0.008	−0.362	−0.007	−0.039	−0.366
C_9	−0.476	−0.733	−0.362	−0.477	−0.731	−0.362	−0.477	−0.715	−0.366
	Ethyl oxamate			Ethyl oxanilate					
	R	TS-II	P	R	TS-II	P			
C_3	1.049	0.972	0.734	1.108	0.956	0.769			
N_1	−0.930	−0.941	−0.733	−1.037	−0.986	−0.679			
H_2	0.397	0.592	0.427	0.416	0.581	0.419			
O_4	−0.738	−0.943	−0.808	−0.750	−0.830	−0.769			

Table 5. NBO analysis for ethyl oxamate (A), ethyl oxanilate (B) and, ethyl *N*,*N*-dimethyl oxamate (C) thermal decomposition at 400°C. Wiberg bond indexes (B_i), % evolution through the reaction coordinate (%Ev), from MP2/6-31G calculations are shown for reactants *R*, TS-I, TS-II, and products *P*. Mechanism for ethylene formation is identified as TS-I (six-member ring) and mechanism for ethanol formation as TS-II (four-member ring). Average bond index variation (δB_{av}) and Synchronicity parameter (Sy) are also reported

		TS-I							
		C_3–O_5	O_4–C_6	C_6–C_9	C_9–H_{11}	H_{11}–O_5	C_3–O_4	δB_{av}	Sy
A	B_i^R	1.6025	0.8187	1.0294	0.9273	0.0002	0.9553	0.496	0.893
	B_i^{ET}	1.2459	0.2991	1.3486	0.4440	0.2686	1.2909		
	B_i^P	0.9689	0.0011	2.0147	0.0131	0.6692	1.5973		
	%Ev	56.3	63.6	32.4	52.9	40.1	52.3		
B	B_i^R	1.5917	0.8156	1.0296	0.9287	0.0000	0.9587	0.496	0.889
	B_i^{ET}	1.2498	0.2859	1.3498	0.4563	0.2594	1.2989		
	B_i^P	0.9712	0.0011	2.0138	0.0138	0.6655	1.5913		
	%Ev	55.5	65.0	32.5	51.6	39.0	53.8		
C	B_i^R	1.6939	0.8049	1.0304	0.9235	0.0000	1.0346	0.504	0.878
	B_i^{ET}	1.2988	0.2440	1.3740	0.4843	0.2421	1.4313		
	B_i^P	0.9975	0.0009	2.0116	0.0155	0.6566	1.7504		
	%Ev	56.7	69.8	35.0	48.4	36.9	55.4		
		TS-II							
		C_3–O_4	C_3–N_1	N_1–H_2	O_4–H_2				
A	B_i^R	0.9553	1.1680	0.7842	0.0014			0.510	0.882
	B_i^{ET}	0.4298	1.5020	0.2746	0.3399				
	B_i^P	0.0022	2.0525	0.0003	0.7332				
	%Ev	55.1	37.8	65.0	46.3				
B	B_i^R	0.9587	1.1308	0.7632	0.0028			0.472	0.890
	B_i^{ET}	0.4905	1.4136	0.2959	0.3184				
	B_i^P	0.0001	1.9089	0.0000	0.7445				
	%Ev	48.8	36.4	61.2	42.6				

means of the Synchronicity (Sy) concept proposed by Moyano *et al.*[17] defined by the expression:

$$\mathrm{Sy} = 1 - \frac{\left[\sum_{i=1}^{n} |\delta B_i - \delta B_{av}| / \delta B_{av}\right]}{2n - 2}$$

n is the number of bonds directly involved in the reaction and the relative variation of the bond index is obtained from:

$$\delta B_i = \frac{[B_i^{TS} - B_i^R]}{[B_i^P - B_i^R]}$$

where the superscripts *R*, TS, *P*, represent reactant, transition state, and product, respectively.

The evolution in bond change is calculated as:

$$\%\mathrm{Ev} = \delta B_i * 100$$

The average value is calculated from:

$$\delta B_{ave} = 1/n \sum_{i=1}^{n} \delta B_i$$

Bonds indexes were calculated for bonds involved in the reaction changes, that is, for mechanism 1 leading to ethylene formation: C_3—O_5, O_4—C_6, C_6—C_9, C_9—H_{11}, H_{11}—O_5, and C_3—O_4 (TS-I Schemes 1, Fig. 2) and for mechanism 2, leading to ethanol formation: bonds C_3—O_4, C_3—N_1, N_1—H_2, and O_4—H_2 (TS-II Schemes 1, Fig. 3). All other bonds remain practically unaltered during the process.

Calculated Wiberg indexes B_i for reactant, TS and products for ethyl oxamate, ethyl oxanilate, and ethyl *N*,*N*-dimethyl oxamate by paths 1 and 2, allows to examine the progress of the reaction and the position of the TS between reactant and product (Table 5). For ethylene formation, (TS-I) Wiberg indexes show more progress in O_4—C_6 bond breaking (64% for ethyl oxamate, 65% for ethyl oxanilate, and 70% for *N*,*N*-dimethyl ethyl oxamate) while the changes in O3—C5, C_3—O_4, C_9—H_{11} bonds are intermediate in the reaction coordinate (52–56%). Less progress is being observed in C_6—C_9 double bond formation (33–35%) and in H_{11}—O_5 single bond formation (37–40%). Wiberg indexes for ethanol formation (TS-II) reveal that the reaction coordinate with more progress is N_1—H_2 bond breaking, that is, the transference of hydrogen H_2 is the most important process in this mechanism, thus acidity of this hydrogen is relevant.

Synchronicity parameters were calculated for both paths 1 and 2. For ethylene formation (TS-I) from ethyl oxamate, ethyl oxanilate, and ethyl *N*,*N*-dimethyl oxamate the synchronicity parameters reveal a concerted semi-polar process. The relative progress in all reaction

coordinates is very similar for all three substrates rendering alike synchronicity values (Sy = 0.89). This is in accord with the similar TS-I structure, both in distances, angles, and NBO charges as analyzed above, with the exception of the departure from planarity which is greater for ethyl *N*,*N*-dimethyl oxamate. The TS-I structure shows more progress in O_4—C_6 bond breaking compared to other reaction changes. This finding suggests that the polarization of this bond in the sense $O_4^{\delta-}$—$C_6^{\delta+}$ is a determining factor in the gas-phase elimination of ethyl oxamate, ethyl oxanilate and ethyl *N*,*N*-dimethyl oxamate (path 1). For path 2 for ethanol formation (TS-II), the synchronicity parameters are also similar for ethyl oxamate and ethyl oxanilate (Sy = 0.88–0.89). This is characteristic of a concerted semi-polar TS structure. In this case, the more progress in reaction coordinate was observed for N_1—H_2 bond breaking.

CONCLUSIONS

In this investigation we provide theoretical evidence for the thermal decomposition mechanism for ethyl oxamate, ethyl oxanilate, and ethyl *N*,*N*-dimethyl oxamate. The first two substrates decompose by two competitive mechanisms leading to ethylene and ethanol formation. The TS-I for ethylene formation (path 1) from the three substrates is a non-planar six-membered cyclic structure, where the most important factor is the polarization of O_4—C_6 bond (breaking of ester bond). The process is semi-polar concerted, with the hydrogen being transferred located halfway between carbonyl oxygen O_5 and C_9.

The ethanol formation from ethyl oxamate and ethyl oxanilate proceeds through a planar four-membered ring TS-II structure. Calculations suggest that the reaction proceeds in a concerted asynchronous mechanism, where the dominating process is the breaking of N1—H2 bond. This explains the difference in reactivity between ethyl oxamate and ethyl oxanilate, the electron-withdrawing effect of the substituent phenyl makes more acidic the hydrogen (N—H), and consequently the reaction is faster. This mechanism is precluded for ethyl *N*,*N*-dimethyl oxamate because there is no hydrogen on the amide nitrogen. Activation parameters are in reasonable agreement with experimental values for MP2/6-31G level of theory for these substrates. Inclusion of polarization functions not always improves the results. The rate coefficients are of the same order of magnitude following the same sequence observed in the experimental. NBO charges analysis suggests that the polarization of alkyl oxygen–carbon bond, in the sense $O_4^{\delta-}$—$C_6^{\delta+}$, is determining factor in the decomposition process following path 1, and N_1—H_2 bond breaking is the most relevant process in path 2.

REFERENCES

1. Herize A, Domínguez RM, Rotinov A, Nuñez O, Chuchani G. *J. Phys. Org. Chem*. 1999: **12**: 201–206.
2. Chacin EV, Tosta M, Herize A, Domínguez RM, Alvarado Y, Chuchani G. *J. Phys. Org.Chem*. 2005: **18**: 539–545.
3. Taylor R. *Int. J. Chem. Kinet*. 1987: **19;** 709–713.
4. Taylor R. *Int. J. Chem. Kinet*. 1991: **23;** 247–250.
5. Córdova T, Rotinov A, Chuchani G. *J. Phys. Org. Chem*. 2004: **17;** 148–151.
6. Gaussian 98, Revision A.3, Frisch MJ, Trucks GW, Schlegel HB, Scuseria GE, Robb MA, Cheeseman JR, Zakrzewski VG, Montgomery JA, Jr., Stratmann RE, Burant JC, Dapprich S, Millam JM, Daniels AD, Kudin KN, Strain MC, Farkas O, Tomasi J, Barone V, Cossi M, Cammi R, Mennucci B, Pomelli C, Adamo C, Clifford S, Ochterski J, Petersson GA, Ayala PY, Cui Q, Morokuma K, Malick DK, Rabuck AD, Raghavachari K, Foresman JB, Cioslowski J, Ortiz JV, Stefanov BB, Liu G, Liashenko A, Piskorz P, Komaromi I, Gomperts R, Martin RL, Fox DJ, Keith T, Al-Laham MA, Peng CY, Nanayakkara A, Gonzalez C, Challacombe M, Gill PMW, Johnson B, Chen W, Wong MW, Andres JL, Gonzalez C, Head-Gordon M, Replogle ES, Pople JA. Gaussian, Inc: Pittsburgh, PA, 1998.
7. McQuarrie D. *Statistical Mechanics*, Harper & Row: New York, 1986.
8. Foresman JB, Frish Æ. *Exploring Chemistry with Electronic Methods* (2nd Edn). Gaussian, Inc: Pittsburg PA, 1996.
9. Benson SW. *The Foundations of Chemical Kinetics*, Mc-Graw-Hill: New York, 1960.
10. Rotinov A, Dominguez RM, Córdova T, Chuchani G. *J. Phys. Org. Chem*. 2005, **18**: 616–624.
11. (a) O'Neal HE, Benson SW. *J. Phys. Chem*. 1967, **71**: 2903–2921; (b) Benson SB. *Thermochemical Kinetics*, Mc-Graw John Wiley & Sons: New York, 1968.
12. Lendvay G. *J. Phys. Chem*. 1989; **93**: 4422–4429.
13. Reed AE, Weinstock RB, Weinhold F. *J. Chem. Phys*. 1985; **83**(2): 735–746.
14. Reed AE, Curtiss LA, Weinhold F. *Chem. Rev*. 1988; **88**: 899–926.
15. Wiberg KB, *Tetrahedron* 1968; **24**: 1083–1095.
16. Gaussian NBO version 3.1.
17. Moyano A, Periclas MA, Valenti E. *J. Org. Chem*. 1989; **54**: 573–582.